



## Concept and development of ITER divertor thermography diagnostic

R. Reichle<sup>a,\*</sup>, Ph. Andrew<sup>b</sup>, C. Balorin<sup>a</sup>, B. Brichard<sup>c</sup>, S. Carpentier<sup>a</sup>, Y. Corre<sup>a</sup>, M. Davi<sup>a</sup>, R. Daviot<sup>a</sup>, C. Desgranges<sup>a</sup>, J.L. Gardarein<sup>a</sup>, E. Gauthier<sup>a</sup>, D. Guilhem<sup>a</sup>, S. Gicquel<sup>b</sup>, A. Herrmann<sup>d</sup>, D. Hernandez<sup>e</sup>, M. Jouve<sup>a</sup>, Ch. Le Niliot<sup>g</sup>, Th. Loarer<sup>a</sup>, A. Martin<sup>b</sup>, J.P. Martins<sup>a</sup>, J.-B. Migozzi<sup>f</sup>, J.P. Patterlini<sup>a</sup>, C. Pocheau<sup>a</sup>, F. Rigollet<sup>g</sup>, H. Roche<sup>a</sup>, J.M. Traveré<sup>a</sup>

<sup>a</sup>CEA, IRFM, F-13108 Saint-Paul-lez-Durance, France

<sup>b</sup>ITER-IT, Joint Work Site, c/a CEA-Cadarache, St. Paul-lez-Durance 13108, France

<sup>c</sup>SCK•CEN, EURATOM Ass. Belgium, Boeretang 200, B-2400 Mol, Belgium

<sup>d</sup>EURATOM Ass. IPP-Garching, Boltzmannstr. 2, Garching, Germany

<sup>e</sup>PROMES CNRS 8521, Centre Felix Trombe, BP5, Odeillo, F-66125 Font Romeu, France

<sup>f</sup>JBM Optique, 11 Avenue de la Division Leclerc, 92310 SEVRES, France

<sup>g</sup>Ecole Polytechnique Universitaire de Marseille, I.U.S.T.I, UMR CNRS No. 6595, Technopôle de Château Gombert, 5 Rue Enrico Fermi, 13453 Marseille cedex 13, France

### ARTICLE INFO

PACS:  
07.57.Ty  
07.60.Vg  
42.79.-e  
52.70.-m

### ABSTRACT

The conceptual and technological development of ITER divertor thermography approaches the aim to provide measurements for machine protection and physics studies even for the case of an eventual change to metallic targets. This requires not only the use of spectrally resolved imaging thermography but also the use of various additional calibration and precision measurement tools such as pyroreflectometry and the use of the photothermal effect. The question of the optical transport through the divertor port is resolved in a compromise with justification for both conventional and fibre elements. The remote handling sequence for such a device is demonstrated. The next steps to take are outlined.

© 2009 Elsevier B.V. All rights reserved.

### 1. Introduction

The temperature of the divertor target plates needs to be surveyed to avoid damage. Power deposition is subject of physics studies in ITER. These aims require to measure surface temperatures over a large temperature range (200–3600 °C) with high spatial resolution (3 mm) and high temporal resolution (2 ms in the range 200–1000 °C, 20 μs above 1000 °C). This can not be provided by the Infrared (IR) instruments in the port plugs [1] but requires an IR diagnostic inside the divertor cassette. An earlier proposal is based on an inverse spectrometer approach [2]. Here we compare two other conceptual studies which allow to observe each target point with spectral resolution in a significant IR wavelength range. One of the justifications for this approach is that in a situation where the radiation of black-bodies of different temperatures (as with hot dust spots on colder targets) are merged within a single measurement channel one can determine the dominating part of the temperature distribution by an analysis of the spectral radiance distribution [1,3–7]. Spectral analysis may also help to distinguish the expectedly high bremsstrahlung signal from thermal radiation of the target [8]. This approach may be sufficient in a

pure carbon environment with near blackbody behaviour but not for temperature measurements on metallic surfaces with low and changing emissivity. We consider choice and integration issues of novel diagnostic elements that might help in that situation. Finally, maintenance and remote handling procedures of the diagnostic are presented before outlining next steps to take.

### 2. Comparison of studies using fibres or conventional optical transport elements

Different concepts for ITER divertor thermography were studied by the IPP Garching and the CEA-Cadarache. The main difference is the transport via conventional optics or via fibres through the divertor port. A comparison of the two approaches is given in Table 1. The CEA has studied the front-end design for the 2005 divertor [8] and the 2007 divertor (Fig. 1) [1] – the IPP study is (Fig. 2) for the 2005 divertor. All designs use the pumping hole of the cassette for optical access and a combination of focusing and reflecting mirrors at the front-end behind small apertures to look at the inner and the outer target and another flat mirror in the middle of the cassette to reunite these two views. The IPP-design front-end is smaller since the aperture of the system is only F/5.2 which keeps the diameter of conventional optical transport in the divertor duct small whereas the CEA system is at F/2.2 which matches the large

\* Corresponding author.

E-mail address: [roger.reichle@cea.fr](mailto:roger.reichle@cea.fr) (R. Reichle).

numerical aperture of the optical fibres, without requiring more room in the divertor duct. The CEA-design has as particular feature a Cassegrain telescope at the entrance of the divertor duct which couples the light into the fibres. The IPP-design has as particular feature additional mirrors at the top of the divertor to view the lower part of the targets. The recent CEA-design (Fig. 1) includes a cooling solution. The cooling circuit of the cassette is used for cooling the diagnostic box inside the divertor cassette and the mirrors inside the box can be branched off the cooling circuit of the diagnostic box.

One of the main questions concerning the fibres had been their radiation hardness. The CEA has searched with the SCK•CEN Mol for radiation hard IR fibres [9,10] with the results that high purity silica core (HPSC) fibres (in the wavelength range 1–2.3  $\mu\text{m}$ ) and sapphire fibres (1–2.8  $\mu\text{m}$ ) are considered as probably usable up to the divertor port/cassette transition. Micro-structured pure silica fibres are promising to give access to transmission windows

of a spectral width of 0.5  $\mu\text{m}$  at wavelengths up to 3.5  $\mu\text{m}$  [11]. These fibres are of interest as illumination transport for the laser methods described in Section 3. ZrF<sub>4</sub> fibres (1–4  $\mu\text{m}$ ) are only usable outside the cryostat [10].

The conventional transport through the divertor port could be made either by mirrors or radiation hard lens combinations.

The comparison between the two approaches (Table 1) does not give a clear advantage of one approach over the other. A compromise could be to use close to the divertor cassette exclusively conventional elements and to combine conventional and fibre transport in the rest of the duct.

### 3. Choice and integration of novel diagnostic elements

Thermography on metallic targets – as in a future ITER tungsten divertor – requires knowledge of the emissivity of the target. The

**Table 1**  
Comparison of fibre and conventional solution. Rating scheme: xxx means better than xx and x; x(x) means that it depends on some details explained in the text box whether it is x or xx.

Criteria	Fibres in the duct	Mirrors or lenses in the duct
Compliance with specs	xx	xx
Radiation hardness and degradation of optical components	<ul style="list-style-type: none"> <li>xx</li> <li>High purity silica core (HPSC) fibres, micro-structured pure silica (MSPS) fibres and sapphire fibres are usable in NIR–MIR range (with possible exception of duct front-end). The glass length is larger than for an equivalent lens solution</li> </ul>	<ul style="list-style-type: none"> <li>Mirrors xxx lenses x(x)</li> <li>IR material choice for lenses not radiation hardness validated yet</li> <li>For lenses at least two materials necessary. In the NIR one material (pure silica) is OK: xx–second material is a problem: x</li> <li>Antireflection coatings on lenses can cause additional problems</li> </ul>
RAMI: Reliability (including robustness against displacement) availability maintainability inspectability	<ul style="list-style-type: none"> <li>xx(x)</li> <li>Self alignment of fibres (if suitable connector: xxx)</li> <li>The image transfer by fibres is very flexible and needs defined optical conditions only at the interfaces to the entrance and exit system</li> <li>Exchange in two stages – see robotics scheme</li> <li>Lowest possible number of optical surfaces</li> <li>Reference fibres</li> </ul>	<ul style="list-style-type: none"> <li>x(x)</li> <li>Careful alignment needed</li> <li>Parts of the relay optics can be built stable against misalignment</li> <li>Critical point: interface between the different relay stages (when in situ alignments proven: xx)</li> <li>Same robotic exchange scheme</li> <li>Higher number of surfaces to (keep) clean</li> <li>Unused parts of the picture for reference</li> <li>xxx (NIR–MIR–LIR)</li> </ul>
Wavelength range	<ul style="list-style-type: none"> <li>xx (NIR–MIR)</li> <li>HPSC: 1–2.3 <math>\mu\text{m}</math>, Sapphire: 1–2.8 <math>\mu\text{m}</math>, MSPS (designable: 1–3.5 <math>\mu\text{m}</math> with 0.5 <math>\mu\text{m}</math> width)</li> <li>Multiple wavelengths can be selected inside the transmission window of the fibres. Fibres allow particular flexible high spectral resolution measurements</li> </ul>	<ul style="list-style-type: none"> <li>A pure mirror solution is most flexible for wavelength selection and spectral measurements – in particular as it allows using fibres for high spectral resolution and filters for high spatial resolution simultaneously. If lenses are chosen in the divertor port similar restrictions apply as for fibres (NIR–MIR)</li> </ul>
Bandwidth and sensitivity	<ul style="list-style-type: none"> <li>xx</li> <li>The bandwidth and the detection wavelength are selectable over a wide wavelength range</li> </ul>	<ul style="list-style-type: none"> <li>xx</li> <li>The bandwidth and the detection wavelength are free selectable and can be adapted: MIR (3–5 <math>\mu\text{m}</math>) or LIR (8–12 <math>\mu\text{m}</math>) waveband with filter width of <math>\Delta\lambda \approx 10\% \lambda</math> for good performance</li> </ul>
Luminosity and optical performance $d\Omega \times \tau \times \Delta\lambda$	<ul style="list-style-type: none"> <li>xxx</li> <li>High luminosity: F/2.2 for fibres</li> <li><math>4 \times 10^{-4} \times 1 \mu\text{m} \times 0.44</math> (mirrors) <math>\times 0.015</math> (LWL) = <math>2.6 \times 10^{-6} \mu\text{m}</math></li> </ul>	<ul style="list-style-type: none"> <li>xx</li> <li>Medium luminosity: F/5.2 for conventional transport</li> <li><math>2 \times 10^{-6} \times 1 \mu\text{m} \times 0.14 = 2.8 \times 10^{-7} \mu\text{m}</math></li> </ul>
Compactness and reduction of neutron streaming	<ul style="list-style-type: none"> <li>xxx</li> <li>The cross section of the fibre bundle (500 fibres) is comparable to cross section required for mirror relay optics albeit at &gt;5 times more light throughput with fibres. Fibres can follow curved ducts and the aspect ratio of the cross section can be changed. Maximum reduction of neutron streaming</li> </ul>	<ul style="list-style-type: none"> <li>x Mirrors xx lenses</li> <li>The free cross section has to be in the order of <math>20 \times 30 \text{ cm}^2</math></li> <li>Neutron shielding needs to bend the optical axis. This can be done with the existing mirrors in the optical path</li> </ul>
Versatility (other cassettes)	(x) Potentially usable for cassettes not in line with the duct	–
Use for active thermography measurements	xxx Active measurements use fibres to transport the illumination light and the collected light	x Conventional optics could be used for the collection path of active measurements
Multi purpose use (other diagnostics)	<ul style="list-style-type: none"> <li>x</li> <li>Usable by other diagnostics, restrictions in usable wavelength</li> </ul>	<ul style="list-style-type: none"> <li>xx</li> <li>Usable by other diagnostics</li> </ul>
Cooling	xx Fibres should be cooled close to cassette – easy to implement	<ul style="list-style-type: none"> <li>xxx Mirrors x lenses</li> <li>Mirrors need less cooling and are easier to cool</li> </ul>

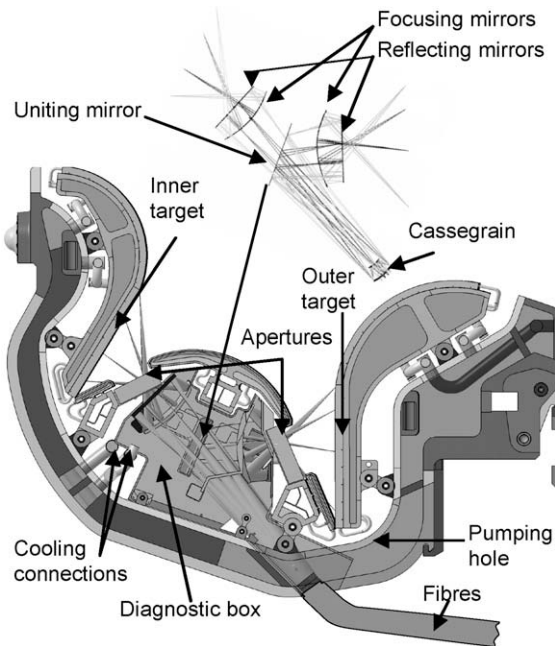


Fig. 1. CEA front-end solution for divertor 2007 – with inset of optical design.

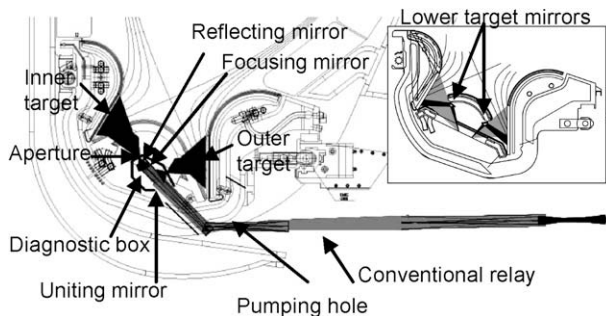


Fig. 2. IPP solution for 2005 divertor and optical relay. Reflecting mirror, focusing mirror and aperture are annotated only for inner target, but exist symmetrically also for outer target.

emissivity will be different from a black body – and even different from a grey body and changing in time. Such emissivity measurements can be provided by the pyroreflectometry method (Section 3.1), which uses laser illumination. To extrapolate such point-like measurements to areas not reached by that method we propose hyperspectral imaging (Section 3.2), which contains spectral information, useful for this extrapolation. To overcome serious reflection and bremsstrahlung problems photothermal methods, also using lasers, are proposed (Section 3.3). The laser methods complement each other. We would preferably use fibres to transport the laser light close to the divertor cassette and then use mirrors to illuminate the target and the normal optical chain described in Section 2 for the associated measurements.

### 3.1. Multicolour pyroreflectometry

This method uses lasers at two or more wavelengths to illuminate the target. The reflected light and the thermal emission at these wavelengths are measured separately. From the reflected light, one can deduce the emissivity and thus determine the true temperature from the thermal emission measurement. This has been successfully demonstrated on Tungsten targets [12,13] by

using near infrared lasers of about 0.1 W to measure temperatures above 700 °C over a distance of a few meters. The use of imaging detectors like the two colour camera mentioned above and light sources in the mid infrared range would allow to cover larger parts of the target and to measure at lower temperatures with less perturbation by the bremsstrahlung. Since the fibre question is presently only solved for the range 2–3.5  $\mu\text{m}$  it would be interesting to continue radiation hardness research for fibres with a transmission range extending to longer wavelengths.

### 3.2. Hyperspectral imaging

We consider two complementary solutions for hyperspectral imaging: either spatially resolving fibre bundles and imaging IR spectrometers as pioneered by Tore Supra (for spectral analysis) [3] or two colour 2D IR cameras (e.g. from SOFRADIR, France, 640 \* 512 pixels HgCdTe, two spectral ranges 3.4–4.2  $\mu\text{m}$  and 4.4–4.8  $\mu\text{m}$ ) – for large area coverage. An ideal compromise would be the combination of both methods by observation of a subsection of the area seen by the camera via beamsplitter and fibre bundles connected to a higher resolving imaging spectrometer.

### 3.3. Photothermal methods

The photothermal methods use either pulsed or modulated laser light to heat up the target. The increase in temperature is measured by two-colour thermography [14]. The status of laboratory experiments towards tokamak application is described in [15]. The required laser power is at least 2–3 orders of magnitude higher than for the pyroreflectometry method. The illumination wavelength can be in the NIR range, where suitable lasers and radiation hard fibres are available. The measurement can be made in the MIR range with the systems described in Section 2.

## 4. Maintenance and remote handling

Tore Supra and JET experience [16] incites to use black-bodies, and other in situ calibration tools including thermocouples in the target and regular mirror cleaning to maintain an accurate security system. For the CEA-design a remote handling sequence has been studied for installation and exchange. The scheme should also be applicable for the IPP-design. The sequence is depicted Fig. 3. The first step is to install the divertor cassette equipped with the diagnostic front-end while the rest of the diagnostic is still in the transfer cask system (Fig. 3(a)). The second step is to install an additional front shield element for the first part of the optical relay (Fig. 3(b)). The third step is the installation of the diagnostic rack which is equipped with the first part of the optical relay (Fig. 3(c)). The second part of the optical relay is then inserted with a separate extension part (Fig. 3(d)). Finally the closure plate is attached which is equipped with the feed-through for the optical relay (Fig. 3(e)).

## 5. Discussion outlook and conclusion

The present solution needs to be adapted to the newest divertor cassette design and the connector between cassette and relay needs to be designed in detail. This work should be accompanied by calculations of the radiation reduction by the front shield (Fig. 3(b)). Initial reflection simulation work [17] needs to be intensified. For power deposition calculations it is necessary to determine the thermal characteristics of deposits on the surface. No additional tools are proposed for this since thermocouples in the

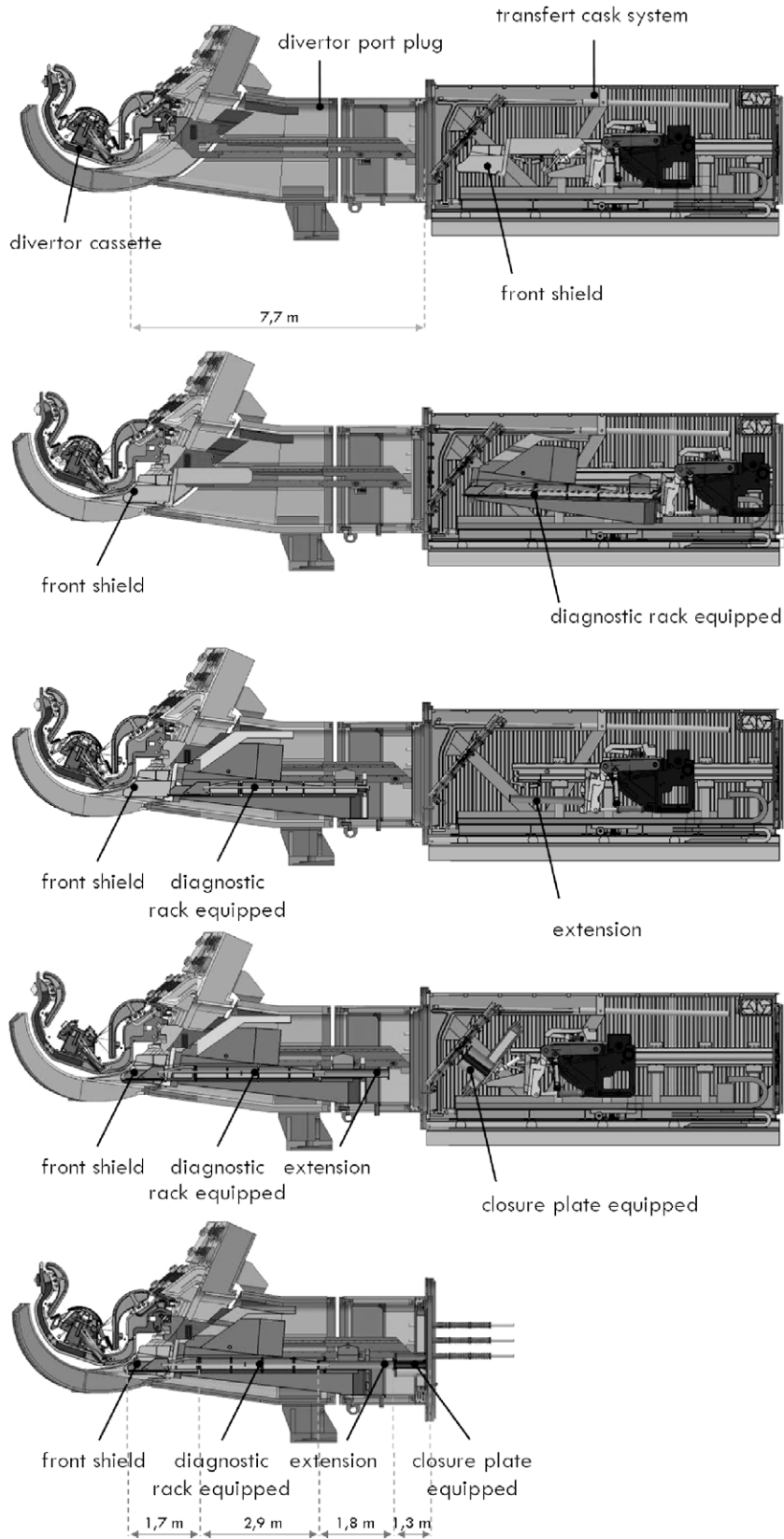


Fig. 3. Remote handling installation sequence.

target and photothermal methods suffice. We arrive at becoming reasonably confident that with the ensemble of methods proposed here, properly interfaced with each other, it is possible to answer

to the ITER requirements even in the case of a change to tungsten as target material. A compromise solution using fibres and conventional elements seems interesting.

## Acknowledgements

This work, supported by the European Communities under the contract of Association between EURATOM/CEA-Cadarache, was carried out within the framework of the European Fusion Development Agreement contract EFDA 06-1429 D4.1. The views and opinions expressed herein do not necessarily reflect those of the European Commission.

## References

- [1] R. Reichle et al., Concept and development of instruments for ITER thermography, in: F.P. Orsitto et al. (Eds.), *Burning Plasma Diagnostics*, AIP, New York, 2008, p. 226.
- [2] K. Itami, T. Sugie, G. Vayakis, *Rev. Sci. Instrum.* 75 (10) (2004) 4124.
- [3] R. Reichle et al., *Rev. Sci. Instrum.* 75 (10) (2004) 4129.
- [4] E. Delchambre, R. Reichle, R. Mitteau, et al., *J. Nucl. Mater.* 337–339 (2005) 1069.
- [5] D. Hildebrandt et al., *J. Nucl. Mater.* 337–339 (2005) 1064.
- [6] A. Herrmann et al., *Phys. Scripta* T111 (2004) 98.
- [7] S. Fougerolle et al., 15 Cong. Franç. de Therm., 29 Mai–1 Juin, Île de Embiez, France, 2007, p. 837.
- [8] R. Reichle et al., in: *Proceedings of the 32nd EPS Conference on Plasma Physics*, ECA, vol. 29C, 2005, P4.083.
- [9] R. Reichle, B. Brichard, F. Escourbiac, et al., *J. Nucl. Mater.* 363–365 (2007) 1466.
- [10] R. Reichle et al., Gamma irradiation test of IR optical fibres for ITER thermography, in: F.P. Orsitto (Ed.), *Burning Plasma Diagnostics*, AIP, New York, 2008, p. 325.
- [11] M. Antkoviak, PhD Thesis, Vrije Universiteit Brussel, Brussels, Belgium, 2007.
- [12] D. Hernandez et al., *Fusion Eng. Design* 83 (2008) 672.
- [13] F. Lott et al., these Proceedings.
- [14] Th. Loarer, F. Brygo, E. Gauthier, et al., *J. Nucl. Mater.* 363–365 (2007) 1450.
- [15] V. Grigороva et al., *J. Nucl. Mater.* 390–391 (2009) 1097.
- [16] J-L. Gardarein et al., *Int. J. Therm. Sci.* 48 (1) (2009) 1.
- [17] D. Guilhem, R. Reichle, H. Roche, *QUIRT* 3 (2) (2006) 155.